PURDUE
UNIVERSITY

A Comparison of Nodal- and Mesh-Based Magnetic Equivalent Circuit Models

H. Derbas, J. Williams[2], A. Koenig[3], S. Pekarek
Department of Electrical and
Computer Engineering

Purdue University
[2]Caterpillar, [3]Hamilton-Sundstrand

April 7, 2008

Outline

- Magnetic Equivalent Circuit (MEC) Modeling

- Alternative MEC Formulations
  - Nodal-based
  - Mesh-based

- Comparison of Numerical Properties

PURDUE UNIVERSITY

MEC Model of Claw-Pole Machine

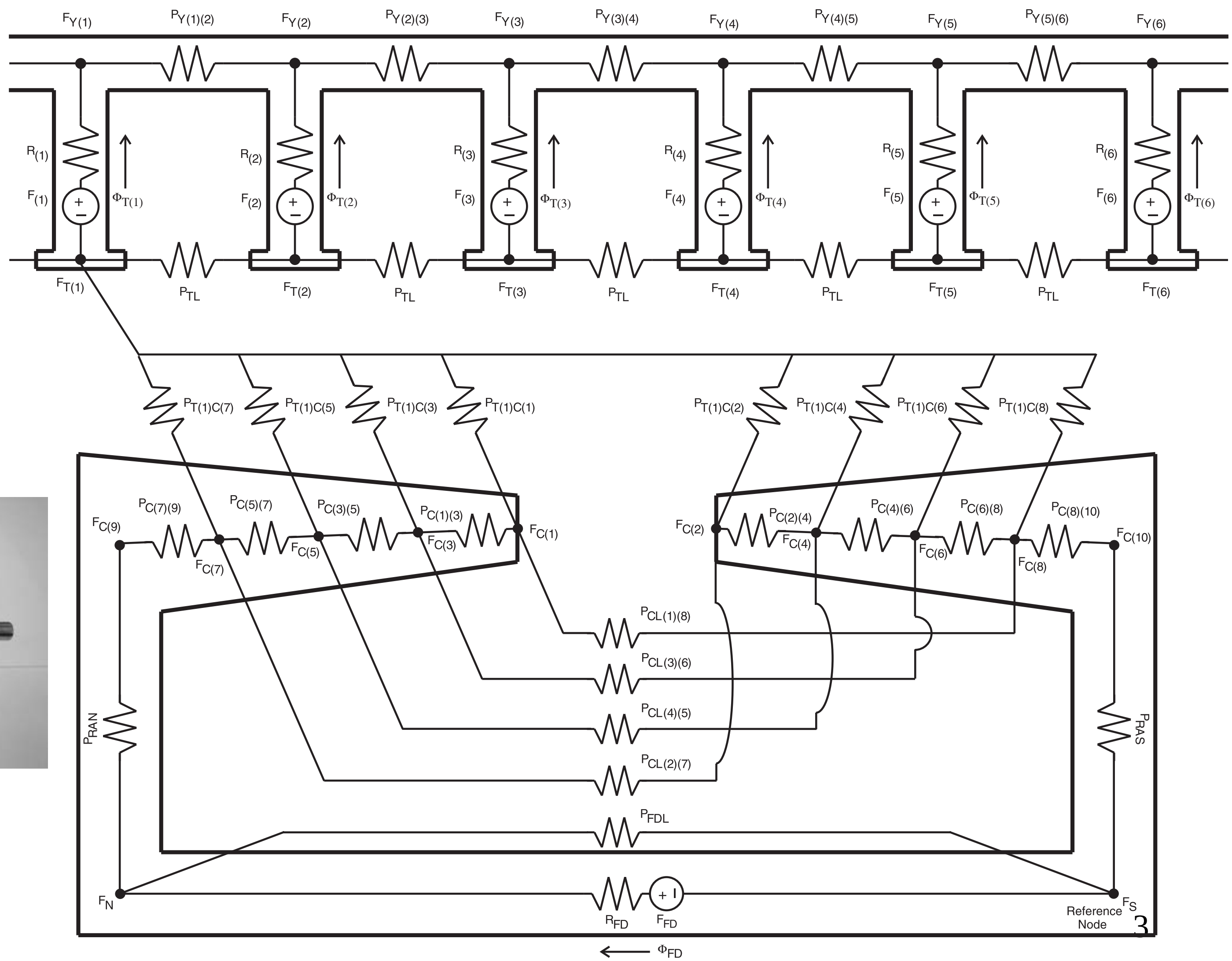

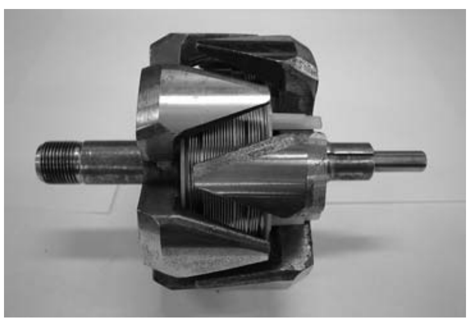

MEC Sources

- Magnetomotive Force
  - Result of Ampere's current Law
  - Represents effects of winding currents
  - Incorporates winding layout
  - Similar to a voltage source

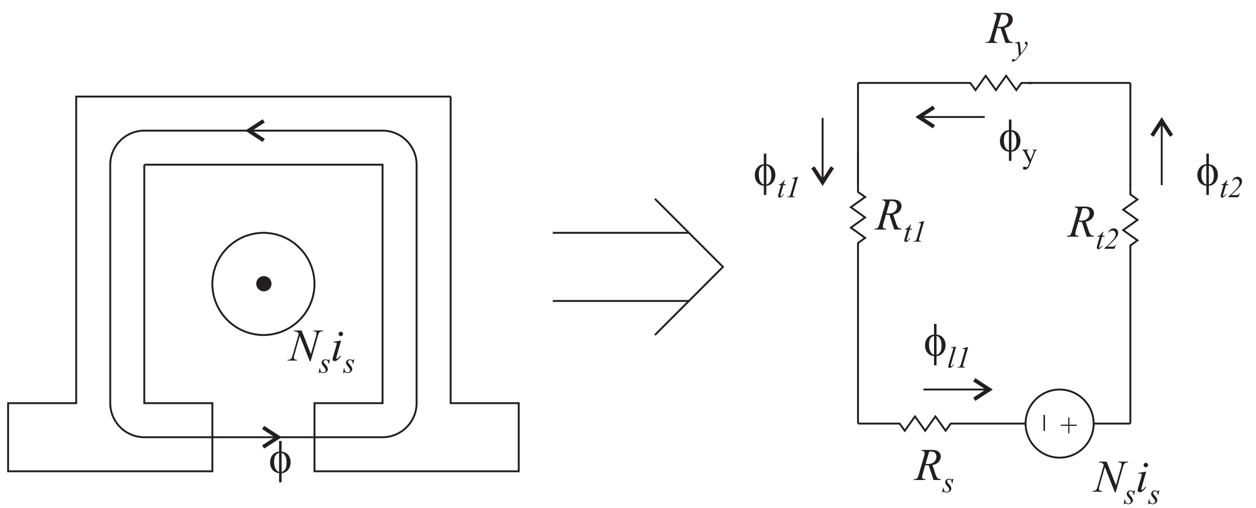

MEC Flux Tubes

- Flux Tubes
  - Shape determined by engineering judgment
  - Establish topology of MEC network
  - Incorporate geometry of the machine

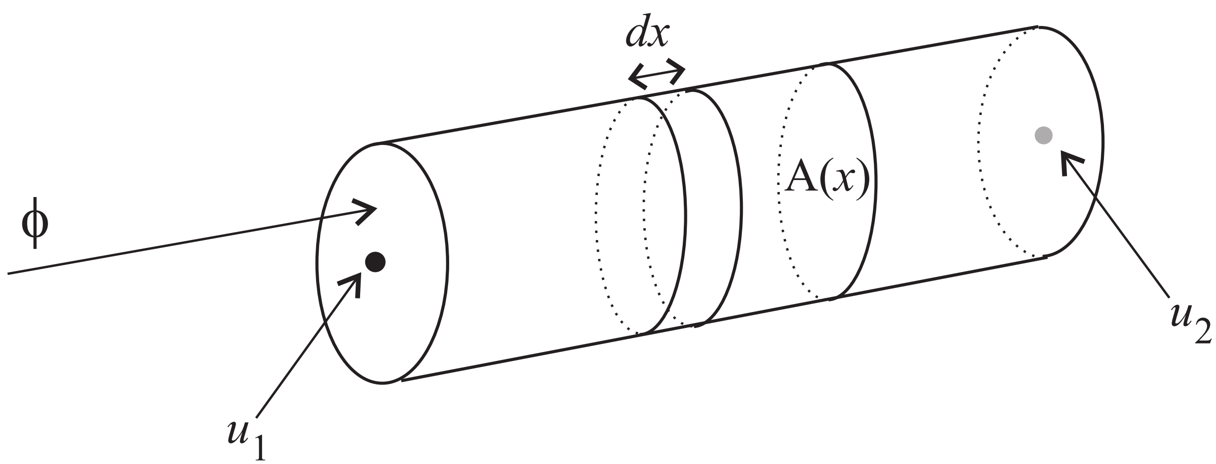

Node Potentials and Reluctance

- Magnetic Scalar Potentials
  - Represent node potentials
- Reluctance
  - Calculated from geometry of flux tube
  - Similar to resistance
  - Allows for effects of magnetic saturation

$$R = \int \frac{dx}{\mu(x)A(x)}$$

PURDUE UNIVERSITY

Example MEC-Based Design Program

```
%----------------------------------------------------------------------------
% Stator Input Data
%----------------------------------------------------------------------------
OD     = 0.12985;   % STATOR OUTER DIAMETER, m
ID     = 0.09662;   % STATOR INNER DIAMETER, m
GLS    = 26.97e-3;  % STATOR STACK LENGTH, m
DBS    = 4.98e-3;   % STATOR YOKE DEPTH, m
SFL    = 0.99;      % STACKING FACTOR
H0     = 0.64E-3;   % STATOR SLOT DIMENSION, m
H1     = 0.0;       % STATOR SLOT DIMENSION, m
H2     = 1.3e-3;    % STATOR SLOT DIMENSION, m
B0     = 2.4617e-3; % STATOR SLOT DIMENSION, m
SYNR   = 2.4e-3;    % STATOR YOKE NOTCH RADIUS, (weight calculation only),
SLTINS = 2.997e-4;  % SLOT INSULATION WIDTH, m
G1     = 0.305e-3;  % MAIN AIR GAP LENGTH, m
SAWG   = 13.75;     % WIRE GUAGE OF ARMATURE WINDING, 1.29e-3
TC     = 11.0;      % NUMBER OF TURNS PER COIL
ESC    = 2.54e-3;   % ARMATURE WINDING EXTENSION BEYOND STACK
RSC    = 7.62e-3;   % ARMATURE WINDING RADIUS BEYOND STACK
CPIT   = 3.0;       % COIL PITCH IN TEETH
STW    = 3.86e-3;   % WIDTH OF TOOTH SHANK, m
DENS   = 7872.0;    % DENSITY OF IRON, ROTOR & STATOR, kg/m^3
SLTH   = 0.828e-3;  % STATOR LAMINATION THICKNESS, m
```

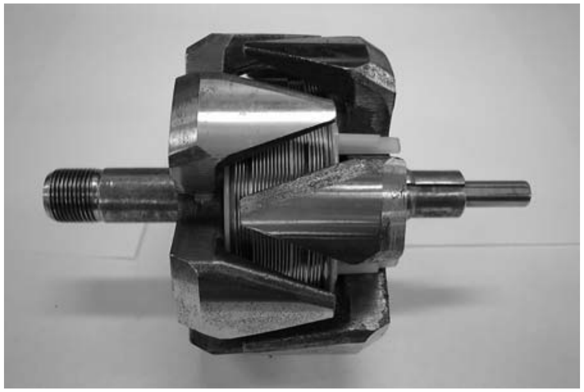

```
%----------------------------------------------------------------------------
% Rotor Input Data
%----------------------------------------------------------------------------
TED    = 12.0e-3;   % ROTOR END DISK THICKNESS, m
DC     = 50.0e-3;   % ROTOR CORE DIAMETER, m
CL     = 28.1e-3;   % ROTOR CORE LENGTH, m
GLP    = 27.0e-3;   % LENGTH OF ROTOR POLE, m
CID    = 51.5e-3;   % FIELD COIL INNER DIAMETER, m
COD    = 74.0e-3;   % FIELD COIL PLASTIC SLOT OUTER
DIAMETER, m
COILW  = 28.0e-3;   % FIELD COIL WIDTH, m
WPT    = 7.39e-3;   % ROTOR TOOTH WIDTH AT TIP OF TOOTH,
arclength, m
WPR    = 27.0e-3;   % ROTOR TOOTH WIDTH AT ROOT OF TOOTH,
arclength, m
HPT    = 2.997e-3;  % ROTOR TOOTH HEIGHT AT TIP OF TOOTH, m
HPR    = 11.38e-3;  % ROTOR TOOTH HEIGHT AT ROOT OF TOOTH,
m
TRAD   = 1.19e-3;   % ROTOR TOOTH BEND RADIUS, m
RP     = 12.0;      % NUMBER OF POLES
TRC    = 306.0;     % FIELD WINDING NUMBER OF TURNS
RAWG   = 19;        % WIRE GUAGE OF FIELD WINDING, 0.813e-3
TFLD   = 48.8;      % HOT FIELD TEMPERATURE, C
TA     = 20.0;      % AMBIENT TEMPERATURE, C
SD     = 17.575e-3; % SHAFT DIAMETER, m
DD     = 58.6e-3;   % DISK DIAMETER (claw V to claw V), m
CW     = 7.697e-2;  % CHAMFER WIDTH, rad
CD     = 3.0*G1;    % CHAMFER DEPTH, m
```

Summary Table

Speed:	1.894e+003	[RPM]		
R Load:	3.440e-001	[Ohm]		
STATOR VARIABLES				
Phase Current:	2.258e+001	[Arms],	3.751e+001	[A op]
Phase Voltage:	1.768e+001	[Vrms],	2.442e+001	[V op]
DC VARIABLES				
Output DC Current:	4.995e+001	[A avg],	1.698e+001	[A ripple]
Output DC Voltage:	1.790e+001	[V avg],	5.841e+000	[V ripple]
FIELD VARIABLES				
Field Current:	4.596e+000	[A avg],	5.164e-001	[A ripple]
Field Voltage:	8.094e+000	[V]		
WEIGHTS				
Teeth Weight:	3.550e-001	[kg]		
Yoke Piece Weight:	4.148e-001	[kg]		
Total Stator Weight:	7.698e-001	[kg]		
Rotor Segment Weight:	1.336e+000	[kg]		
Rotor Core Weight:	3.780e-001	[kg]		
Permenent Magnet Weight:	0.000e+000	[kg]		
Total Rotor Weight:	1.714e+000	[kg]		
Total Magnetic Weight:	2.484e+000	[kg]		
Stator Winding Weight:	5.306e-001	[kg]		
Rotor Winding Weight:	3.455e-001	[kg]		
Total Copper Weight:	8.760e-001	[kg]		
Total Weight:	3.360e+000	[kg]		
EFFICIENCY & LOSS				
Efficiency:	6.172e+001	[%]		
Avg Power In:	1.465e+003	[W]		
Avg Power Out:	9.045e+002	[W]		
Friction & Windage Loss:	1.984e+001	[W]		
Stator Core Loss, Fund:	9.080e+001	[W]		
Stator Core Loss, 3*Fund:	1.980e+000	[W]		
Stator Core Loss, 5*Fund:	5.414e+000	[W]		
Stator Core Loss, 7*Fund:	4.557e-001	[W]		
Rotor Pole Face Loss:	7.993e+001	[W]		
Stator I^2 R Loss (3-PH):	1.274e+002	[W]		
Diode Losses (6):	2.003e+002	[W]		
Field I^2 R Loss:	3.719e+001	[W]		

SHAFT TORQUE		
Avg Torque:	7.389e+000	[Nm]
Ripple Torque:	3.148e+000	[Nm pp]
PEAK MAGNETIC FLUX DENSITY		
Claw Section 1 (tip):	1.140e+000	[T]
Claw Section 3:	1.455e+000	[T]
Claw Section 5:	1.600e+000	[T]
Claw Section 7:	1.788e+000	[T]
Yoke Piece 1:	1.260e+000	[T]
Tooth 1:	1.664e+000	[T]
End Piece:	1.336e+000	[T]
End Disk Piece:	1.378e+000	[T]
Shaft:	1.333e+000	[T]
Core:	1.483e+000	[T]
PEAK AMPERE-TURNS		
Claw Section 1 (tip):	5.865e+000	[A-turn]
Claw Section 3:	2.027e+001	[A-turn]
Claw Section 5:	3.870e+001	[A-turn]
Claw Section 7:	9.008e+001	[A-turn]
Yoke Piece 1:	7.179e+000	[A-turn]
Tooth 1:	5.349e+001	[A-turn]
End Piece:	3.777e+001	[A-turn]
End Disk Piece:	7.190e+001	[A-turn]
Shaft:	1.040e+002	[A-turn]
Core:	1.040e+002	[A-turn]
INDUCTANCE		
Lasfd (mag fundamental):	7.270e-003	[H]
Lasas (average):	4.642e-004	[H]
MISC		
Radial Force:	1.151e+002	[N]
RMS EMF:	2.922e+001	[V]
Stator Slot Fill:	6.032e+001	[%]
Rotor Slot Fill:	7.207e+001	[%]
Stator Resistance:	8.323e-002	[ohm]
Field Resistance:	1.761e+000	[ohm]
Field Hot Temp:	4.880e+001	[C]

Example System for Research Presented Herein

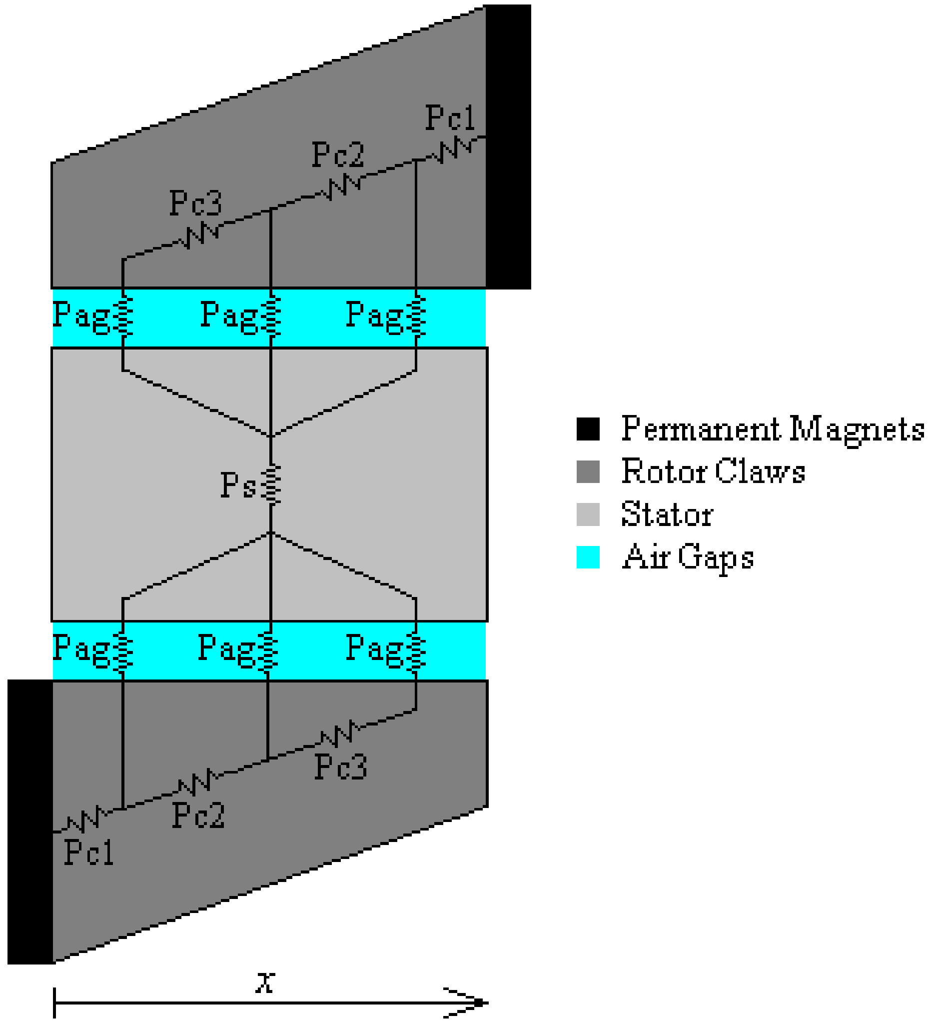

Nodal Analysis of Example

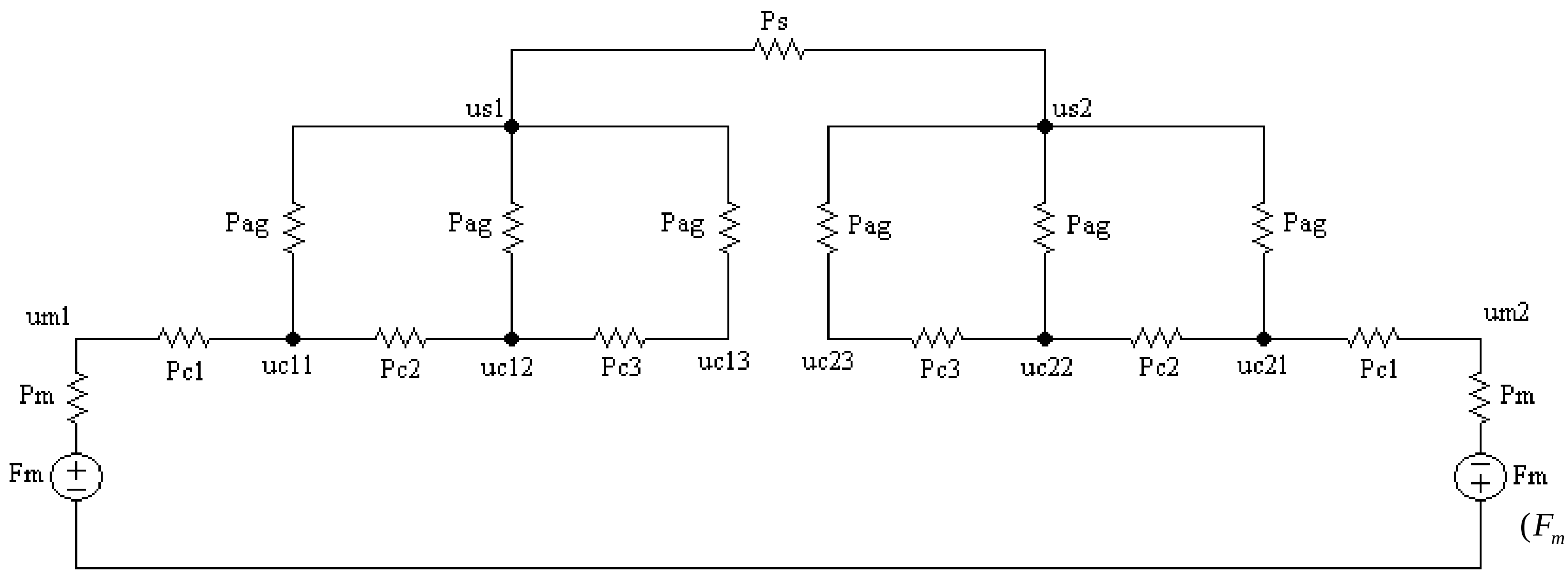

$(F_m = H_c t_{mag})$

$$\mathbf{A}_P \mathbf{u} = \varphi$$

$$\mathbf{u} = \begin{bmatrix} u_{m1} & u_{c11} & u_{c12} & u_{c13} & u_{s1} & u_{s2} & u_{c23} & u_{c22} & u_{c21} & u_{m2} \end{bmatrix}^T$$

$$\varphi = \begin{bmatrix} F_m P_m & 0 & 0 & 0 & 0 & 0 & 0 & 0 & 0 & -F_m P_m \end{bmatrix}^T$$

Nodal-Based Matrices

$$\mathbf{A}_P = \begin{bmatrix} A_{P1} & A_{P2} \\ A_{P2}^T & A_{P4} \end{bmatrix}$$

$$\mathbf{A}_{P1} = \begin{bmatrix} P_m + P_{c1} & -P_{c1} & 0 & 0 & 0 \\ -P_{c1} & P_{ag} + P_{c1} + P_{c2} & -P_{c2} & 0 & -P_{ag} \\ 0 & -P_{c2} & P_{ag} + P_{c2} + P_{c3} & -P_{c3} & -P_{ag} \\ 0 & 0 & -P_{c3} & P_{ag} + P_{c3} & -P_{ag} \\ 0 & -P_{ag} & -P_{ag} & -P_{ag} & 3P_{ag} + P_s \end{bmatrix}$$

$$\mathbf{A}_{P2} = \begin{bmatrix} 0 & 0 & 0 & 0 & 0 \\ 0 & 0 & 0 & 0 & 0 \\ 0 & 0 & 0 & 0 & 0 \\ 0 & 0 & 0 & 0 & 0 \\ -P_s & 0 & 0 & 0 & 0 \end{bmatrix}$$

$$\mathbf{A}_{P4} = \begin{bmatrix} 3P_{ag} + P_s & -P_{ag} & -P_{ag} & -P_{ag} & 0 \\ -P_{ag} & P_{ag} + P_{c3} & -P_{c3} & 0 & 0 \\ -P_{ag} & -P_{c3} & P_{ag} + P_{c2} + P_{c3} & -P_{c2} & 0 \\ -P_{ag} & 0 & -P_{c2} & P_{ag} + P_{c1} + P_{c2} & -P_{c1} \\ 0 & 0 & 0 & -P_{c1} & P_m + P_{c1} \end{bmatrix}$$

Mesh Analysis of Example System

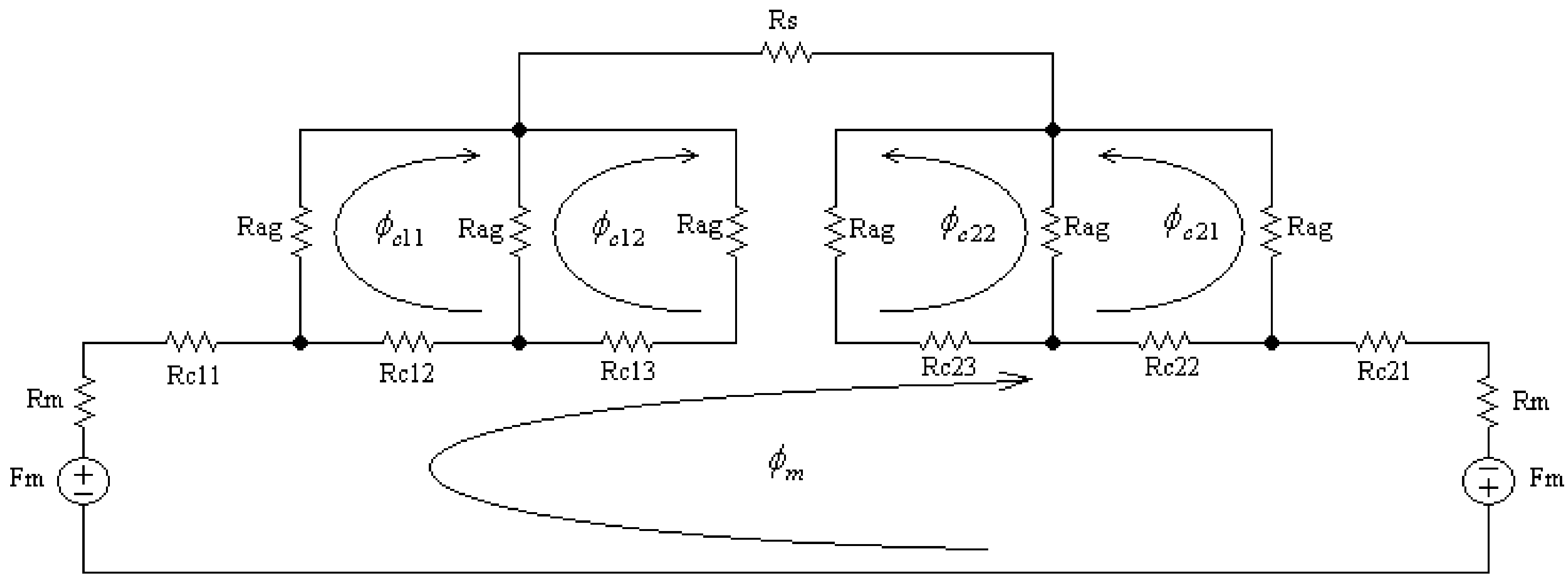

$$\mathbf{A}_R \boldsymbol{\varphi} = \mathbf{F}$$

$$\boldsymbol{\varphi} = \begin{bmatrix} \phi_m & \phi_{c11} & \phi_{c12} & \phi_{c22} & \phi_{c21} \end{bmatrix}^T$$

$$\mathbf{F} = \begin{bmatrix} 2F_m & 0 & 0 & 0 & 0 \end{bmatrix}^T$$

Mesh-Based Matrix

$$\mathbf{A}_R = \begin{bmatrix} R_M & -R_{c12} & -R_{c13} - R_{ag} & R_{c23} + R_{ag} & R_{c22} \\ -R_{c12} & R_{c12} + 2R_{ag} & -R_{ag} & 0 & 0 \\ -R_{c13} - R_{ag} & -R_{ag} & R_{c13} + 2R_{ag} & 0 & 0 \\ R_{c23} + R_{ag} & 0 & 0 & R_{c23} + 2R_{ag} & -R_{ag} \\ R_{c22} & 0 & 0 & -R_{ag} & R_{c22} + 2R_{ag} \end{bmatrix}$$

Modeling Magnetic Materials

Nonlinear – Saturation of Material

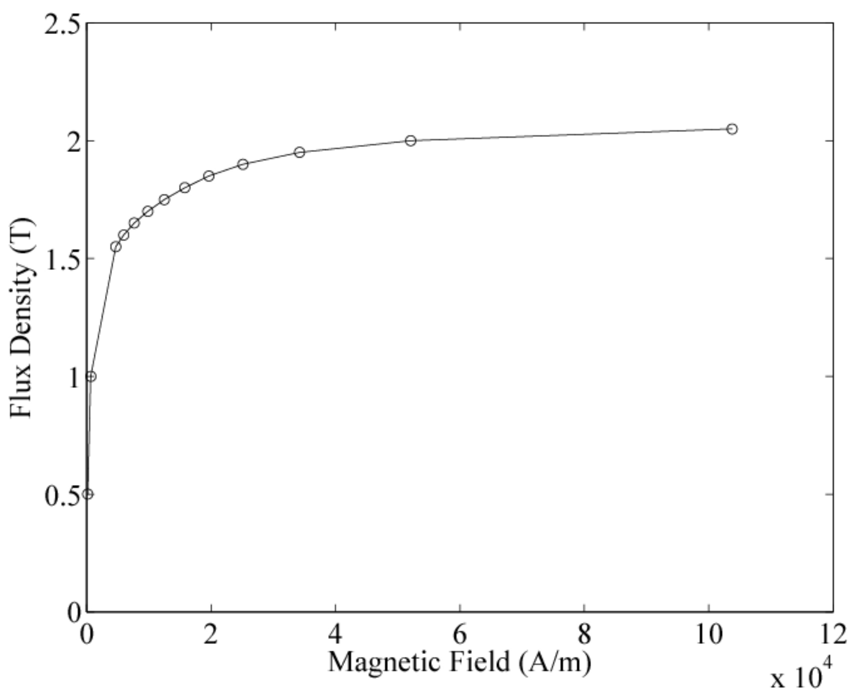

B-*H* Curve

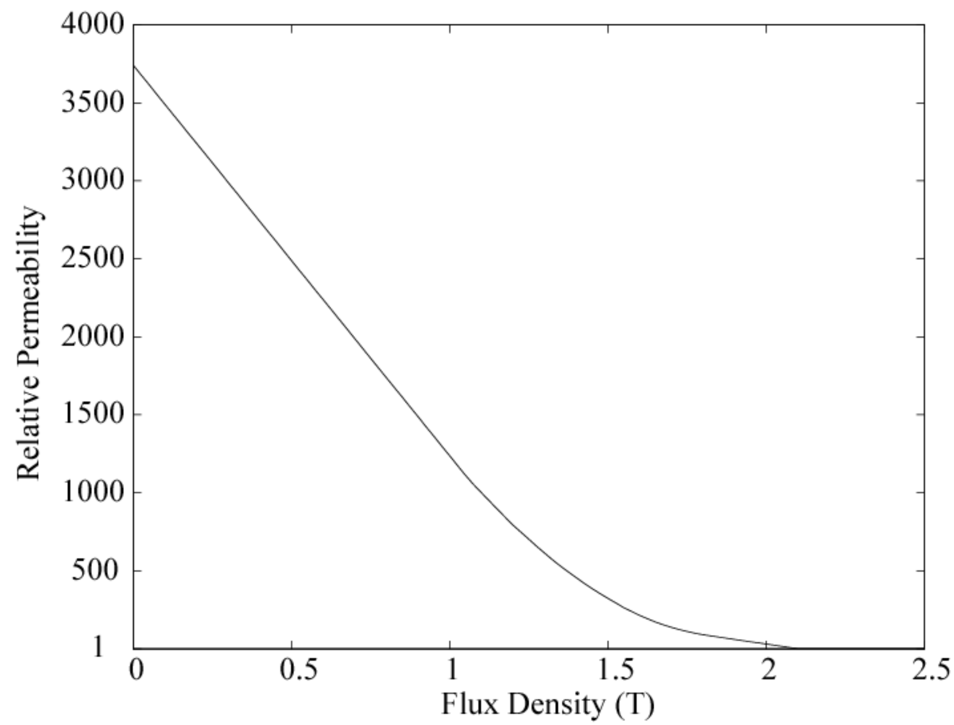

μ –*B* Curve

PURDUE UNIVERSITY

Solving Nodal Formulation

$$f(u) = \mathbf{A}_P \mathbf{u} - \varphi = 0$$

Utilizing Newton Raphson $\mathbf{u_{n+1}} = \mathbf{u_n} - \left[J(\mathbf{u_n}) \right]^{-1} \mathbf{f}(\mathbf{u_n})$

$$f_1(u) = (P_m + P_{c1}) u_{m1} - P_{c1} u_{c11} - F_m P_m = 0$$

$$\Phi_{c1} = P_{c1}(u_{m1} - u_{c11}) \qquad B_{c1} = \frac{\Phi_{c1}}{A_{c1}}$$

$$J_{11} = \frac{\partial f_1}{\partial u_{m1}} = (P_m + P_{c1}) + \frac{\partial P_{c1}}{\partial u_{m1}}(u_{m1} - u_{c11})$$

Closed-form Expression for Jacobian

$$\frac{\partial P_{c1}}{\partial u_{m1}} = \frac{\partial P_{c1}}{\partial \mu_{rc1}} \frac{\partial \mu_{rc1}}{\partial B_{c1}} \frac{\partial B_{c1}}{\partial \Phi_{c1}} \frac{\partial \Phi_{c1}}{\partial u_{m1}} \Rightarrow$$

$$\frac{\partial P_{c1}}{\partial \mu_{rc1}} = \frac{\mu_0 N (l_1 - l_2)}{l_{claw} \ln\left({l_1}/{l_2} \right)} = \frac{P_{c1}}{\mu_{rc1}}$$

$\dfrac{\partial \mu_{rc1}}{\partial B_{c1}}$ from μ-B curve

$$\frac{\partial B_{c1}}{\partial \Phi_{c1}} = \frac{1}{A_{c1}}$$

$$\frac{\partial \Phi_{c1}}{\partial u_{m1}} = \frac{\partial P_{c1}}{\partial u_{m1}} (u_{m1} - u_{c11}) + P_{c1}$$

So, one can establish closed-form expression

$$\frac{\partial P_{c1}}{\partial u_{m1}} = \frac{\alpha \beta \gamma P_{c1}}{1 - \alpha \beta \gamma (u_{m1} - u_{c11})}$$

Solving Mesh Formulation

$$g(\varphi) = \mathbf{A}_R \boldsymbol{\varphi} - \mathbf{F} = 0$$

$$g_1(\varphi) = R_M \phi_m - R_{c12}\phi_{c11} - \left(R_{c13} + R_{ag}\right)\phi_{c12}$$
$$+\left(R_{c23} + R_{ag}\right)\phi_{c22} + R_{c22}\phi_{c21} - 2F_m = 0$$

Rc11, *Rc12*, *Rc13*, *Rc21*, *Rc22*, and *Rc23* are flux-dependent reluctances

$$J_{11} = R_M + \frac{\partial R_{c11}}{\partial \phi_m}\phi_m + \frac{\partial R_{c21}}{\partial \phi_m}\phi_m + \frac{\partial R_{c12}}{\partial \phi_m}\left(\phi_m - \phi_{c11}\right) +$$
$$\frac{\partial R_{c22}}{\partial \phi_m}\left(\phi_m + \phi_{c21}\right) + \frac{\partial R_{c13}}{\partial \phi_m}\left(\phi_m - \phi_{c12}\right) + \frac{\partial R_{c23}}{\partial \phi_m}\left(\phi_m + \phi_{c22}\right)$$

PURDUE
UNIVERSITY

Closed-form Expression for Jacobian

$$\frac{\partial R_{c12}}{\partial \phi_m} = \frac{\partial R_{c12}}{\partial \mu_{rc12}} \frac{\partial \mu_{rc12}}{\partial B_{c12}} \frac{\partial B_{c12}}{\partial \Phi_{c12}} \frac{\partial \Phi_{c12}}{\partial \phi_m} \Longrightarrow \frac{\partial R_{c12}}{\partial \mu_{rc12}} = -\frac{1}{\mu_{rc12}} R_{c12}$$

$\frac{\partial \mu_{rc12}}{\partial B_{c12}}$ Obtained from μ-B curve

$$\frac{\partial B_{c12}}{\partial \Phi_{c12}} = \frac{1}{A_{c12}}$$

$$\frac{\partial \Phi_{c12}}{\partial \phi_m} = -1$$

So, one can establish closed-form expression (much less tedious than permeance-based)

$$\frac{\partial R_{c12}}{\partial \phi_m} = \frac{R_{c12}}{\mu_{rc12} A_{c12}} \frac{\partial \mu_{rc12}}{\partial B_{c12}}$$

Comparison of Nodal and Mesh-Based Formulations

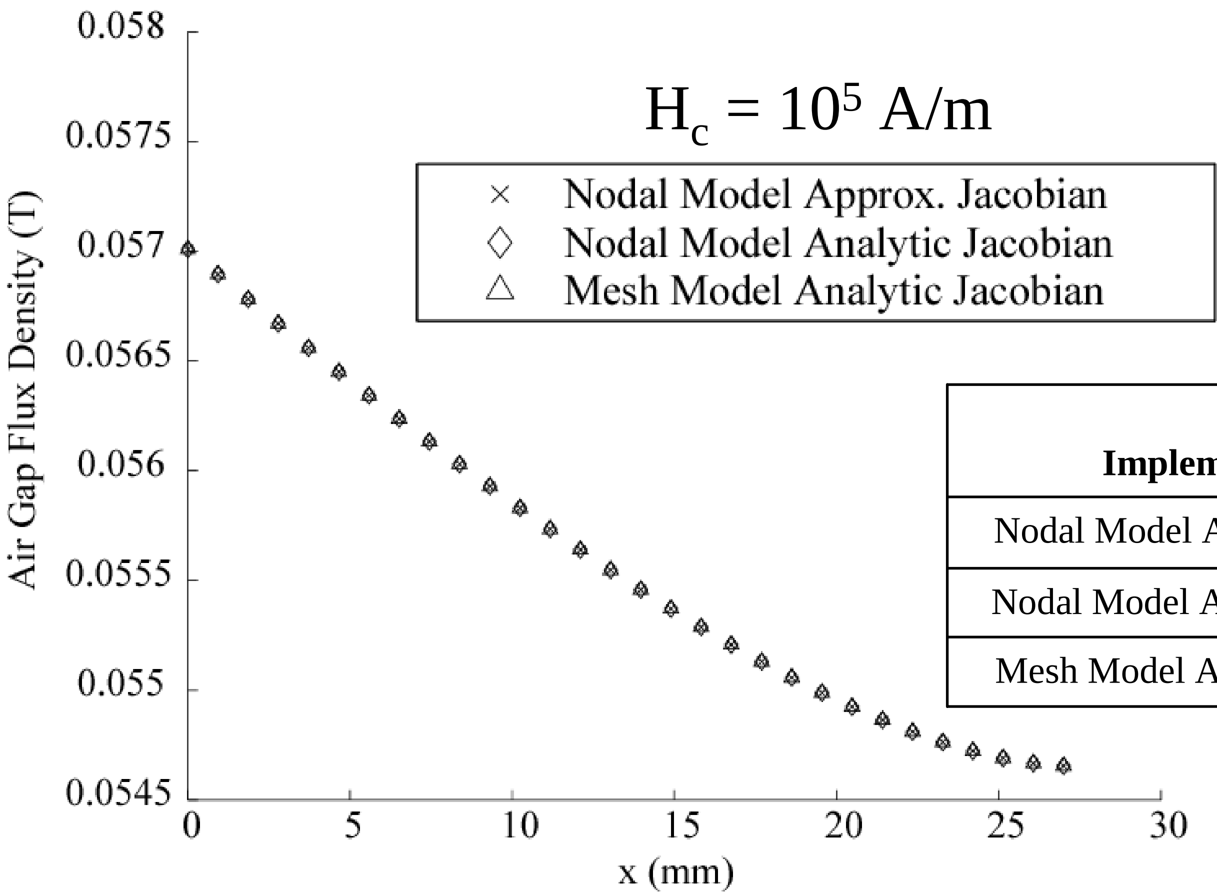

Implementation	Convergence
Nodal Model Approx. Jacobian	3 iterations
Nodal Model Analytic Jacobian	3 iterations
Mesh Model Analytic Jacobian	4 iterations

Comparison of Nodal and Mesh-Based Formulations

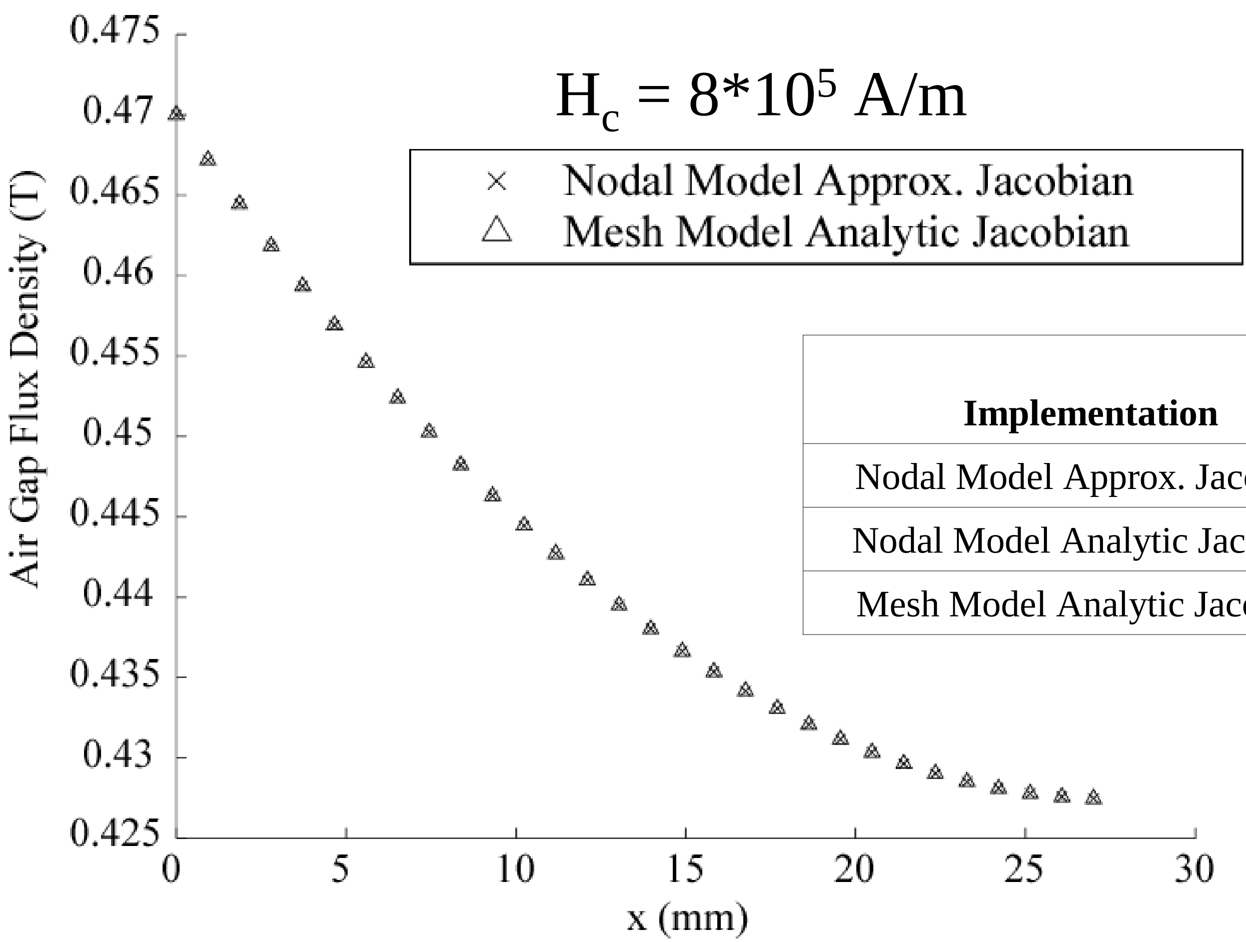

Implementation	Convergence
Nodal Model Approx. Jacobian	5 iterations
Nodal Model Analytic Jacobian	DNC
Mesh Model Analytic Jacobian	5 iterations

Comparison of Nodal and Mesh-Based Formulations

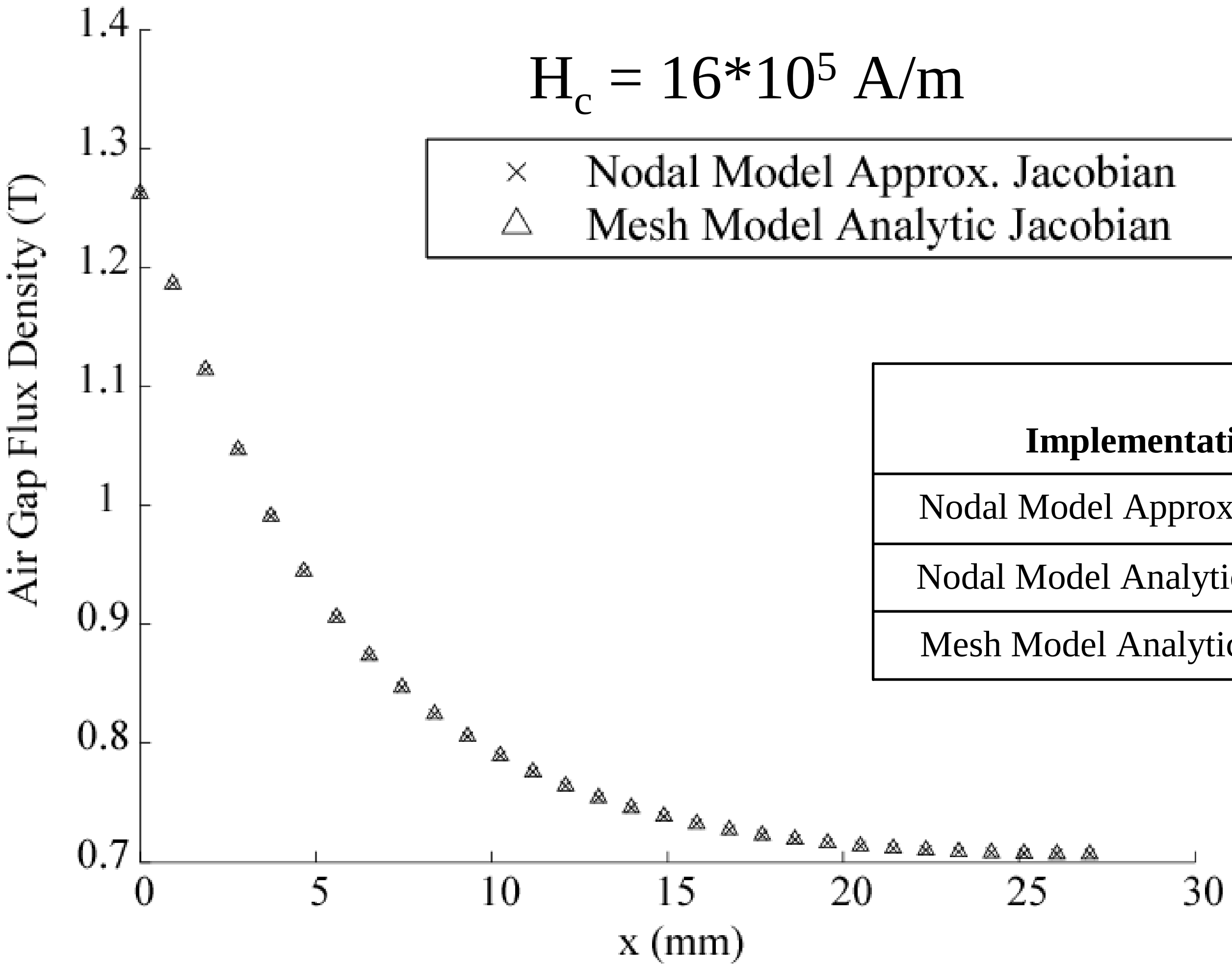

Implementation	Convergence
Nodal Model Approx. Jacobian	53 iterations
Nodal Model Analytic Jacobian	DNC
Mesh Model Analytic Jacobian	6 iterations

PURDUE
UNIVERSITY

Interpretation of Results

$$\mathbf{x}_{\mathbf{n+1}} = \mathbf{x}_{\mathbf{n}} - \left[J\left(\mathbf{x}_{\mathbf{n}}\right)\right]^{-1}\mathbf{f}\left(\mathbf{x}_{\mathbf{n}}\right)$$

Implementation	**Condition Number**
Nodal Model Approx. Jacobian	~ 2 x 10^5
Nodal Model Analytic Jacobian	~ 2 x 10^8
Mesh Model Analytic Jacobian	~ 500

Ill-conditioning mainly due to difference in airgap permeance and claw permeances

PURDUE UNIVERSITY

Scaling to Help?

$$\mathbf{A}_{P1} = \begin{bmatrix} P_m + P_{c1} & -P_{c1} & 0 & 0 & 0 \\ -P_{c1} & P_{ag} + P_{c1} + P_{c2} & -P_{c2} & 0 & -P_{ag} \\ 0 & -P_{c2} & P_{ag} + P_{c2} + P_{c3} & -P_{c3} & -P_{ag} \\ 0 & 0 & -P_{c3} & P_{ag} + P_{c3} & -P_{ag} \\ 0 & -P_{ag} & -P_{ag} & -P_{ag} & 3P_{ag} + P_s \end{bmatrix}$$

$$\mathbf{A}_{P4} = \begin{bmatrix} 3P_{ag} + P_s & -P_{ag} & -P_{ag} & -P_{ag} & 0 \\ -P_{ag} & P_{ag} + P_{c3} & -P_{c3} & 0 & 0 \\ -P_{ag} & -P_{c3} & P_{ag} + P_{c2} + P_{c3} & -P_{c2} & 0 \\ -P_{ag} & 0 & -P_{c2} & P_{ag} + P_{c1} + P_{c2} & -P_{c1} \\ 0 & 0 & 0 & -P_{c1} & P_m + P_{c1} \end{bmatrix}$$

Not in this case

Challenge of Mesh-Based Implementation

- Physical movement between magnetic materials
  - Permeances go to zero with non-overlap
  - Reluctances go to infinity with non-overlap
    - Loops are position dependent

- Not a challenge for stationary magnetics
  - Can use discrete rotor positions for machine design and create set of stationary magnetics

- Recent research has shown promising algorithmic method to automate loop changes

Conclusions

- Nodal-based and Mesh-based MEC have different numerical properties
- Mesh-based has better convergence in Newton Raphson formulations
  - ‘Exact’ nodal formulation of Jacobian highly ill-conditioned
  - Approximate Jacobian better conditioned, but still poor relative to mesh-based
- In cases where motion represented, Mesh-based formulation must deal with infinite reluctance
- Algorithmic means of dealing with infinite reluctance is being considered